COBEM 2023 27TH INTERNATIONAL CONGRESS OF MECHANICAL ENGENEERING

ABCM Brazilian Society of Mechanical Sciences and Engineering
27th ABCM International Congress of Mechanical Engineering
December 04-08, 2023, Florianópolis-SC, Brazil

COB-2023-0552
OPTICAL PERFORMANCE COMPARISON OF TWO CONFIGURATIONS OF LINEAR FRESNEL COLLECTORS RECEIVERS

Patricia Scalco
Jacqueline Biancon Copetti
Mario Henrique Macagnan
Unisinos University, Mechanical Engineering Graduate Program, LETEF, Laboratory of Thermal and Fluid Dynamic Studies, Unisinos Avenue, 950, São Leopoldo, 93022-750, RS, Brazil.
patrscalco@edu.unisinos.br; jcopetti@unisinos.br; mhmac@unisinos.br

André Vitor de Albuquerque Santos
Diogo Canavarro
University of Évora, Renewable Energies Chair, Polo da Mitra da Universidade de Évora, Edifício Ário Lobo de Azevedo, 7000-083 Nossa Senhora da Tourega, Portugal.
avas@uevora.pt; diogocvr@uevora.pt

Jeferson Diehl de Oliveira
FSG-University Center, Center of Innovation and Technology, Department of Mechanical Engineering, Os Dezoito do Forte, 2366, Caxias do Sul, 95020-472, RS, Brazil
jeferson.oliveira@fsg.edu.br; jeferson.physics@gmail.com

Abstract. *The challenges of climate change turn the investment in renewable energy sources crucial. Among these sources, concentrating solar power (CSP) has the potential to play a significant role in the transition to a more sustainable and secure energy future. This study focuses on a Linear Fresnel Reflector (LFR): a CSP technology that uses flat - or slightly - curved mirrors to concentrate sunlight at a focal point, known as the receiver. At the receiver, the sunlight is absorbed and used to generate heat for industrial processes and/or centralized and dispatchable electricity, with the eventual inclusion of thermal storage. The optical characteristics of the receiver configuration vary depending on the system's geometry. This study aims to present an optical analysis for two receiver configurations: (1) trapezoidal receiver cavity with a multi-tube system; and (2) Compound Parabolic Concentrator (CPC) secondary concentrator with an evacuated tube. For each configuration, a ray-tracing procedure was carried out. From this, it was possible to define the optical efficiency, the Incidence Angle Modifier (IAM) curves, and the Concentrated Acceptance Product (CAP). This analysis shows that the receiver configuration is a critical component of LFR systems, as it directly affects the overall performance. The findings help to understand the optical characteristics of the receiver of the LFR system, show alternatives to optimize the receiver configuration, and to improve its design.*

Keywords: *linear Fresnel reflector, optical analysis, Incidence Angle Modifier, Concentrated Acceptance Product.*

1. INTRODUCTION

Concentrated solar power (CSP) is a renewable energy technology that utilizes mirrors to concentrate the sunlight into a small area, generating heat that can be used to produce electricity (Zhu et al., 2014). Linear Fresnel Reflector (LFR) is one of the existing CSP technologies that concentrate the radiation onto an absorber tube positioned in a focal point. Through the absorber tube flows a Heat Transfer Fluid (HTF), such as water, thermal oil, molten salt, air, or nanofluids (Bellos et al., 2018; Bellos et al., 2019; Famiglietti and Lecuona, 2021; Sá et al., 2018).

The mirrors in the LFR system are arranged in parallel rows mounted in a way that tracks the sun throughout the day (see Figure 1). The sunlight reflected by the mirrors is focused on the receiver. The receiver is positioned in a fixed height above the mirror field, where the Direct Normal Irradiation (DNI) is concentrated and converted into thermal energy. Additionally, the receiver consists of one or more absorber tubes, which can be either evacuated or non-evacuated, and a second surface to increase the concentrated energy. The design of this secondary surface can vary depending on the LFR system project. It can either be a receiver cavity with internally painted walls using a selective, or high-temperature resistant ink, or it can be a secondary concentrator. In the latter case, the inner walls of the receiver are made of a reflective material, causing multiple reflections of sunlight, until the rays converge to the absorber tube or diverge into the surroundings. Due to this second surface the target width of the reflected sunlight is enlarged, and the radiation can be more effectively intercepted by the absorber, resulting in lower heat loss and a higher concentration ratio (Prasad et al., 2017).

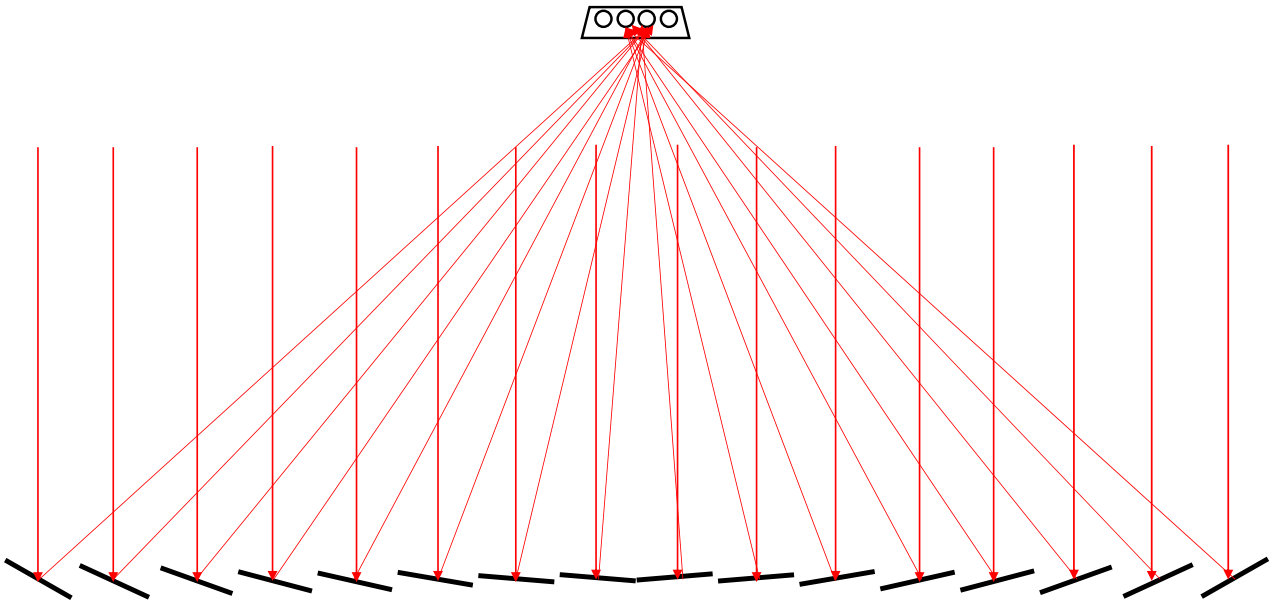

Figure 1. Linear Fresnel Reflector representation.

The secondary concentrator surface geometry can be trapezoidal (Facão and Oliveira, 2011), or a more complex geometry can be used, such as Compound Parabolic Concentrator (CPC) (Ma et al., 2021; Boccalatte et al., 2022; Garg et al., 2023), Compound Elliptical Concentrator (Canavarro et al., 2016), or other polynomial surfaces (Abbas et. al, 2018). Besides that, the secondary concentrator acts like an insulation cover for the absorber tube, reducing the convective heat loss (Prasad et. al, 2017).

The position and dimensions of the receiver in an LFR system are critical to its performance and are defined through optical simulations that calculate the absorbed heat flux at the receiver (Santos et al., 2021a).

This study presents a study case of a LFR prototype located at UNISINOS University which has fourteen rows of mirrors, with a concentrating area of 25.98 m² (4.33 m x 6 m), and a receiver with a trapezoidal cavity with a multi-tube mounting, and an opening area of 1.52 m² (0.254 m x 6 m). From this, an optical analysis is proposed to compare the absorbed heat flux for two specific configurations of receivers: (1°) a trapezoidal cavity with multi-tube mounting; (2°) a CPC secondary concentrator with an evacuated tube. Furthermore, an optimization of the primary field was applied using the Gap Angle concept (Santos et al., 2021b) – which represents the maximum deviation that the reflected ray from the edge of each mirror can undergo without being blocked by the adjacent mirror. Therefore, the center position of each mirror will be determined based on ensuring that the edge ray of the previous mirror is not blocked. The gap angle, θ_{gap}, is calculated by the Equation 1, in which C_{max} represents the maximum solar concentration.

$$\theta_{gap} = \sin^{-1}\left(\frac{1}{C_{max}}\right) \tag{1}$$

Moreover, another concentration factor is important to understand the behavior of LFR system: the Concentrated Acceptance Product (CAP), which determines how much a solar concentrator is closer to an ideal one (Santos et al., 2021a), and it is given by the Equation 2, in which C is the concentration factor, and θ_{accep} is the half-acceptance angle.

$$CAP = C \sin\theta_{accep} \tag{2}$$

In the ray-tracing approach used, the θ_{accep} is calculated considering static mirror rows, without the tracking system, and defining the incidence angle in which the concentrator collects 90 % of the power (Santos et al., 2021). Moreover, C is given by the ratio between the mirror field area (A_{mirror}) and the receiver aperture area ($A_{receiver}$) (Equation 4).

$$C = \frac{A_{mirror}}{A_{receiver}} \tag{3}$$

As a tool for the optical analysis and to carry out the ray tracing procedure, the software SolTrace will be used (Wendelin and Jorgensen, 2018).

2. METHODOLOGY

This section will detail how the optical analysis was carried out, and what were the stages of the methodology adopted. Figure 2 shows the stages of the methodology used for the optical analysis. The first step is to establish the configuration of the mirror field and the receiver of the LFR system. From this, the ray tracing procedure is applied. With this, it is possible to verify and analyze the optical efficiency and the IAM (Incidence Angle Modifier) curves. The optical efficiency is defined by the ratio between the absorbed flux and the total flux incident in the mirror field. The IAM, in turn, is defined by the fraction between the optical efficiency for a given angle of incidence of solar radiation and the optical efficiency for a normal incidence of radiation.

The next step consists of optimizing the mirror field through the gap angle concept, θ_{gap}. Then, a new ray tracing procedure is applied, but now considering a CPC (Compound Parabolic Concentrator) secondary surface and an evacuated tube as a new receiver configuration.

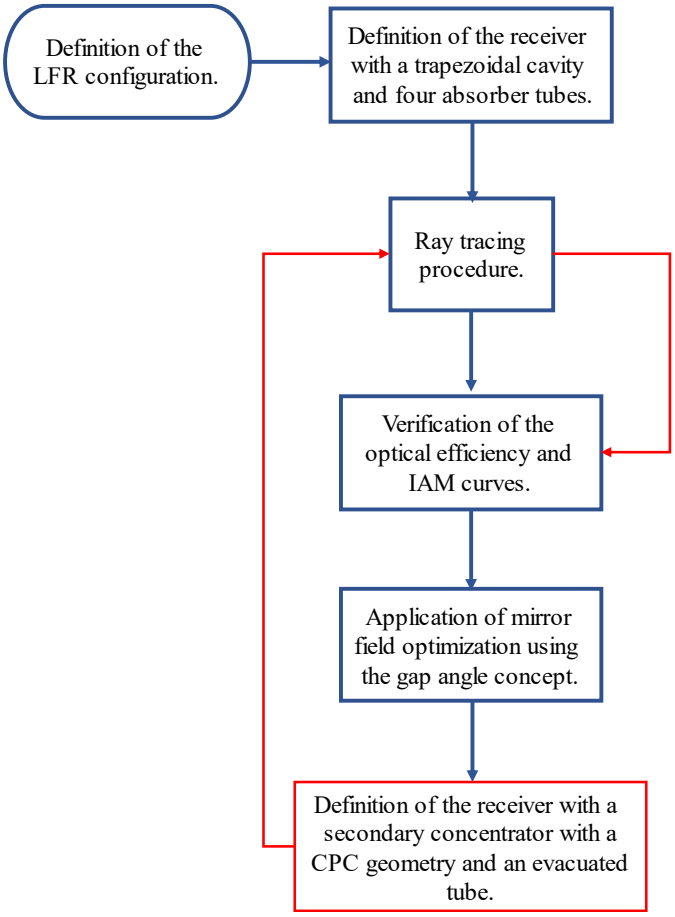

Figure 2. Flowchart of optical analysis steps.

As above described, the first step of this study was the application of a ray tracing procedure for a receiver with a trapezoidal cavity with four absorber tubes. The receiver aperture is 254.05 mm, and the absorber tubes have 33,4 mm in diameter. The inner walls of the trapezoidal cavity and absorber tubes have an absorptivity of 0.95 and 1.0, respectively. Figure 3 shows the geometrical representation of the receiver with a trapezoidal cavity and its dimensions.

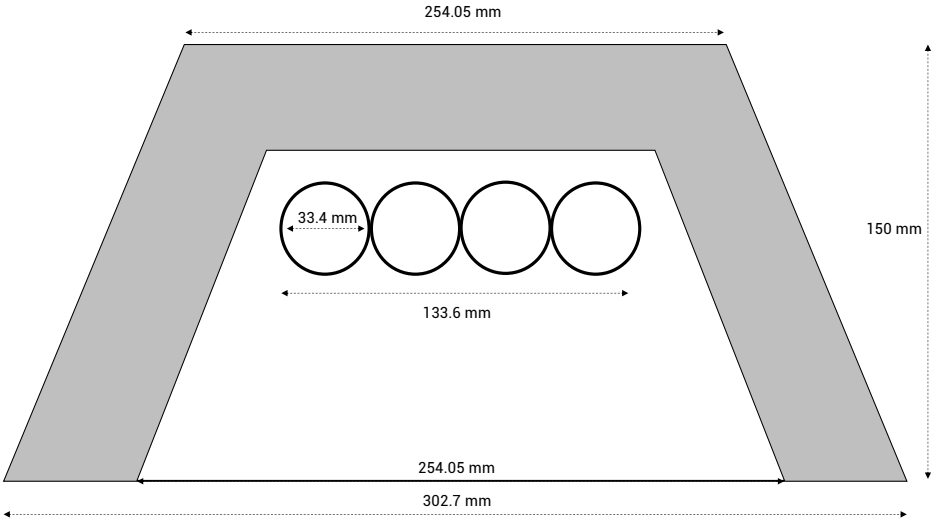

Figure 3. Geometrical representation for the receiver with a trapezoidal cavity used in the ray tracing procedure.

The receiver is positioned 3 m above the mirror field, which has 14 rows of mirrors with 1 cm between each row. In addition, each row of mirror has 30 cm of width 6 m of length – that is divided in 3 mirrors of 2 m. Thus, the mirror field is composed of 42 mirrors. Table 2 specifies the geometric dimensions of the mirror field.

Table 1. Linear Fresnel reflector mirror field characteristics for the first ray tracing simulation.

Description	Dimension
Rows of mirrors	14
Mirror width	300 mm
Spacing between rows of mirrors	10 mm
Mirror length	6 m
Mirror field area	25,98 m²

After the first ray-tracing procedure, the gap angle concept was applied in the LFR mirror field, in which the best position for the mirror center depends on the behavior of the incident ray on the mirror edge. In other words, the mirror position must be the one in which the deviation of the reflected ray on the mirror edge must not focus on the back side of the adjacent mirror. Considering this, the distribution of the mirrors does not need to be symmetric: the distance between the mirror rows is not the same, and neither is the width of the mirrors.

After the optimization, a new ray tracing procedure is applied in the receiver, but now for a receiver with a secondary concentrator with a CPC geometry, and an evacuated tube. In this case, the evacuated tube is the Schott PTR®70, specific for solar applications. Figure 4 shows the geometric representation of the receiver for the second ray tracing procedure, in which the receiver aperture is 300 mm, and the evacuated tube has a diameter of 70 mm.

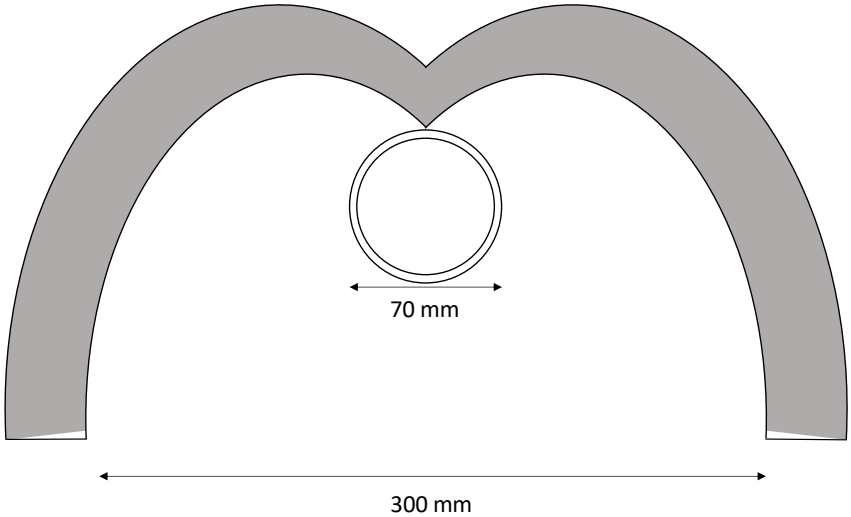

Figure 4. Geometric representation of the receiver with a CPC secondary concentrator and an evacuated tube.

3. RESULTS

This section is divided into three parts: the first part will present the results of the ray-tracing procedure for the receiver with a trapezoidal cavity and four absorber tubes; the second part will be dedicated to the results obtained through the gap angle concept applied to be mirror field; and finally, the third part of the results section will present the ray-tracing procedure applied with the mirror field optimized and for the receiver with a CPC secondary concentrator with an evacuated tube.

3.1 Ray-tracing procedure for the trapezoidal receiver cavity with four absorber tubes

The dimensions used in this procedure were defined in Tables 1. It is important to highlight that in this case, all mirrors have the same dimensions, and all rows of mirror have the same distance between each other. The reflectivity of the primary mirrors is 0.92. The dimensions of the receiver were previously indicated, and the resulting opening area is 1.524 m². Considering this, the concentration ratio, *C*, is 17.05.

Through the simulation, the optical efficiency for a normal incidence is 77% - considering a Direct Normal Irradiation (DNI) 1000 W/m² - the acceptance angle, θ_{accep}, is 0.79°, and the Concentration Acceptance Product (*CAP*) is 0.24. Figure 5 shows the relation between the transversal Incidence Angle Modifier (IAM) and the incidence angle.

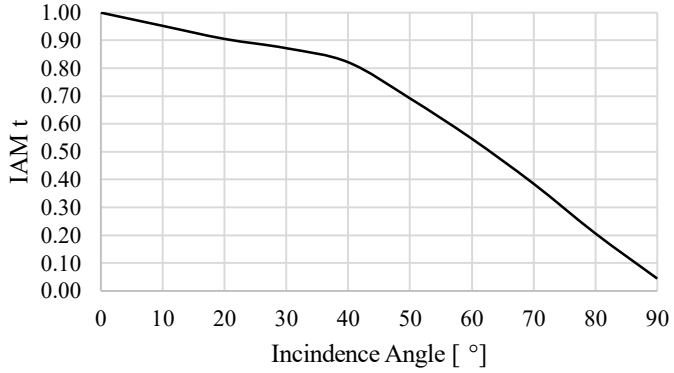

Figure 5. Relation between Transversal Incidence Angle Modifier (IAM) and the Incidence Angle for the receiver with a trapezoidal cavity and four absorber tubes.

3.2 Application of Gap Angle Concept on LFR mirror field

By applying the gap angle concept, the concentrating field is reconfigured to find the best position and spacing between the rows of mirrors. This concept is applied considering that the incident ray in the edge of each mirror must not reflect in the back side of the adjacent mirror – in this case, the parameters are defined considering the maximum deviation that the incident ray can suffer without being blocked by the adjacent mirror. Tables 2 shows the results of the spacing between rows of mirrors after applying the gap angle concept. Before the application of gap angle concept, the spacing between mirror was the same, 1 cm. About the width of mirrors, it remained the same before and after the application of gap angle concept – 30 cm. What has changed is the number of rows of mirrors, which have been reduced from 14 to 12.

Table 2. Spacing between rows of mirrors after the application of gap angle concept.

Position of spacing between rows of mirrors	Spacing After Gap Angle [cm]
Between the 1° and 2°	11.6
Between the 2° and 3°	7.6
Between the 3° and 4°	4.8
Between the 4° and 5°	2.7
Between the 5° and 6°	1.3
Between the 6° and 7°	6.5
Between the 7° and 8°	1.3
Between the 8° and 9°	2.7
Between the 9° and 10°	4.8
Between the 10° and 11°	7.6
Between the 11° and 12°	11.6

3.3 Ray tracing procedure for the CPC secondary concentrator with an evacuated absorber tube

The dimensions and configuration of the receiver with the CPC secondary concentrator and an evacuated tube were described in methodology section. The mirror field configuration was obtained by applying the gap angle concept, and it is detailed in section 3.2. The reflectivity of the mirrors and the inner surface of the secondary concentrator is 0.92 and 0.95, respectively. Considering this, the concentration factor, *C*, is 14.43 – regarding the fact that the concentration factor is a relation between the mirror field area and the receiver opening area.

For this configuration, and through the ray tracing procedure, the optical efficiency, η_0, for a normal incidence is 63 % - considering a Direct Normal Irradiation (DNI) 1000 W/m² -, the θ_{accep} is 0.32°, and the *CAP* is 0.08. Figure 6 shows the graphic with the curve that represents the relation between the transversal IAM and the incidence angle.

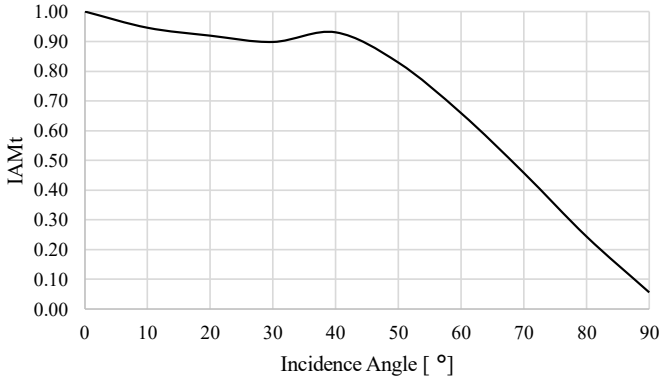

Figure 6. Relation between Transversal Incidence Angle Modifier (IAM) and the Incidence Angle for the receiver with a CPC secondary concentrator and an evacuated tube.

4. DISCUSSION

The optical efficiency under a normal incidence for the receiver with a trapezoidal cavity and for the receiver with a CPC secondary concentrator is 77 % and 63 %, respectively. Even though the receiver with the secondary concentrator has been simulated with an optimized mirror field, its optical efficiency is lower. The hypothesis is that when the simulation for the receiver with the CPC secondary concentrator was carried out, the receiver height was considered the same as the trapezoidal receiver. The receiver at a higher height would imply a wider acceptance angle, increasing the number of reflected rays absorbed by the absorber tube.

The IAM curves conform to the behavior of characteristics curves for LFR systems. Even the acceptance angle and the CAP are lower for the LFR configuration with the CPC secondary concentrator – 0.32° and 0.08, respectively – the IAM curve has a better performance, considering it has a less steep drop.

Moreover, the number of mirror rows has decreased after applying the gap angle concept – from 14 to 12 rows of mirrors – and as a consequence, the spacing between mirrors increased, and the optical losses due to blocking and shading decreased. Besides this, even though the efficiency for the LFR system with the CPC secondary concentrator has lower efficiency, it must be considered that in this mounting there is only one absorber tube whereas, for the receiver with a trapezoidal cavity, there were four absorber tubes. Furthermore, in theoretical and conceptual terms, the CPC secondary concentrator type has a better optical performance than other configurations once its advanced optical physics applied are designed to absorb the maximum quantity of radiation.

The hypothesis for the lower optical efficiency and the lower CAP after the application of the gap angle concept is that the primary field area is the same before and after the optimization: Before, we had a field full of mirrors with little distances between rows of mirrors and, consequently a high portion of blocking and shading losses. On the other hand, when the gap angle concept was applied, the distance between mirrors increased, and the width of mirrors remained the same – keeping the same mirror field area. Consequently, the number of rows of mirrors decreased (from 14 to 12 rows of mirrors). Even though the optical losses are lower after the gap angle concept, the energy that reaches the absorber is lower.

5. CONCLUSIONS

This study presented an optical simulation of an LFR system for two different configurations of the receiver: trapezoidal cavity and CPC secondary concentrator, and its results have been discussed. Besides that, the gap angle concept was applied in the mirror field as a way to minimize the optical losses due to shading and blocking and, consequently, enhance the number of rays absorbed by the absorber tube. These analyzes were made through a ray tracing procedure using the software Soltrace.

The results have shown that the receiver with the CPC secondary concentrator has a CAP lower than the receiver with the trapezoidal cavity – 0.08 and 0.24, respectively –, besides, the optical efficiency for the first one also is lower – 63 % and 77 %, respectively. Even with lower efficiency, the receiver with the CPC secondary concentrator proves to have a better performance when we consider its concept and the behavior of IAM curves, which maintain the highest values when increasing the angles of incidence.

There is, therefore, space for future research to further deepen this analysis: Other simulations could include an increase in mirror field and the analysis of other optical losses, such as end-line losses and the influence of cosine effect on optical efficiency over the year to optimize even more the performance of LFR systems, and the variation of the height of the receiver (to find its optimal position). These studies have the potential to contribute to the continuous advancement and improvement of LFR technology, making it more efficient and viable in practical applications.

6. ACKNOWLEDGEMENTS

The author Patricia Scalco would like to thank the Coordenação de Aperfeiçoamento de Pessoal de Nível Superior – Brasil (CAPES) – Finance code 001, for the finance support. The authors would like to thank the Postgraduate Program in Mechanical Engineering at the UNISINOS University, and the Renewable Energy Chair of the University of Évora.

7. REFERENCES

Abbas, R., Sebastián, A., Montes, M. J., Valdés, M. (2018). Optical features of linear Fresnel collectors with different secondary reflector technologies. Applied Energy, 232, 386-397.

Bellos, E., Tzivanidis, C., & Papadopoulos, A. (2018). Optical and thermal analysis of a linear Fresnel reflector operating with thermal oil, molten salt and liquid sodium. Applied Thermal Engineering, 133, 70-80.

Bellos, E., Tzivanidis, C., & Papadopoulos, A. (2019). Enhancing the performance of a linear Fresnel reflector using nanofluids and internal finned absorber. Journal of Thermal Analysis and Calorimetry, 135, 237-255.

Boccalatte, A., Fossa, M., & Ménézo, C. (2022). Calculation of the incidence angle modifier of a Linear Fresnel Collector: The proposed declination and zenith angle model compared to the biaxial factored approach. Renewable Energy, 185, 123-138.

Canavarro, D., Chaves, J., & Collares-Pereira, M. (2016). A novel Compound Elliptical-type Concentrator for parabolic primaries with tubular receiver. Solar Energy, 134, 383-391.

Famiglietti, A., & Lecuona, A. (2021). Small-scale linear Fresnel collector using air as heat transfer fluid: Experimental characterization. Renewable Energy, 176, 459-474.

Garg, A., Ray, B., Jain, S. (2023). Development of Nusselt number correlation for solar CPC with a tubular receiver. Thermal Science and Engineering Progress, 37, 101553.

Ma, J., Wang, C. L., Zhou, Y., & Wang, R. D. (2021). Optimized design of a linear Fresnel collector with a compound parabolic secondary reflector. Renewable Energy, 171, 141-148.

Prasad, G. C., Reddy, K. S., & Sundararajan, T. (2017). Optimization of solar linear Fresnel reflector system with secondary concentrator for uniform flux distribution over absorber tube. Solar Energy, 150, 1-12.

Sá, A. B., Pigozzo Filho, V. C., Tadrist, L., & Passos, J. C. (2018). Direct steam generation in linear solar concentration: Experimental and modeling investigation–A review. Renewable and Sustainable Energy Reviews, 90, 910-936.

Santos, A. V., Canavarro, D., Horta, P., & Collares-Pereira, M. (2021a). An analytical method for the optical analysis of Linear Fresnel Reflectors with a flat receiver. Solar Energy, 227, 203-216.

Santos, A. V., Canavarro, D., & Collares-Pereira, M. (2021b). The gap angle as a design criterion to determine the position of linear Fresnel primary mirrors. Renewable Energy, 163, 1397-1407.

Schott PTR®70 Receiver. Schott Solar. Available in: https://www.schott.com/pt-br.

Wendelin, T., & Jorgensen, G. (2018). SolTrace. National Renewable Energy Lab.(NREL), Golden, CO (United States).

Zhu, G., Wendelin, T., Wagner, M. J., & Kutscher, C. (2014). History, current state, and future of linear Fresnel concentrating solar collectors. Solar Energy, 103, 639-652.

8. RESPONSIBILITY NOTICE

The authors are the only responsible for the printed material included in this paper.